Nanoparticles in Block-Copolymer Films Studied by Specular and Off-Specular Neutron Scattering[†]

V. Lauter-Pasyuk,*,[‡,§,||] H. J. Lauter,[||] G. P. Gordeev,[⊥] P. Müller-Buschbaum,[‡]
B. P. Toperverg,[⊥,#] M. Jernenkov,[§,||] and W. Petry[‡]

*Technical University München, Physik-Department LS E13, D-85747 Garching, Germany,
Joint Institute for Nuclear Research, 141980 Dubna, Russia, Institut Laue Langevin, B.P. 156,
F-38042, Grenoble, France, Petersburg Nuclear Physics Institute, 188450, Gatchina, Russia,
and Institut für Festkörperforschung, Forschungszentrum Jülich, D-52425 Jülich, Germany*

For the design of multicompositional materials with a spatially defined order of different components symmetric polystyrene(deuterated)-*block*-polybuthyl methacrylate P(Sd-*b*-BMA) lamellar thin films are used as a structure-directing matrix for the nanoparticle arrangement. A P(Sd-*b*-BMA) diblock-copolymer film spontaneously self-assembles upon annealing into a lamellar multilayer and orders the PS-coated nanoparticles, incorporated into the polymer solution prior to annealing, in a periodic lamellar structure. Specular reflection and off-specular neutron scattering were applied to determine the distribution of magnetite Fe_3O_4 nanoparticles in a symmetric P(Sd-*b*-BMA) film with a concentration of the nanoparticles of 7% of the volume fraction. From the experiments on neutron specular reflection and off-specular scattering, we obtained information about the distribution of the nanoparticles within the lamellae and about the distortion of the lamellar order of the copolymer matrix.

Introduction

The engineering of new nanocomposite materials and devices is of considerable current interest. Most of the high-performance composites comprise a macromolecular matrix and metallic or nonmetallic nanoparticles. With change of the chemical composition of the nanoparticles, the properties of the host matrix can be optimized or changed. Some organic/inorganic nanocomposites were designed using self-assembled polymers with following decoration of the surface with metal nanoparticles,[1−3] solution/melt of polymer in hydrocarbon oil,[4] or electrochemical methods.[5] These methods, based on the diffusion process or rigid chemical bonds, result in interesting options of nanoparticle features. However, they do not provide an access to a selective or flexible distribution of assemblies of the nanoparticles inside the polymer matrix. We used self-assembling organic thin lamellar films in which nanoparticles can be incorporated in a controlled way.

The nanocomposite was designed using a template matrix formed with symmetric diblock copolymers. These copolymers spontaneously self-assemble during annealing into a regular lamellar structure.[6] By coating the nanoparticles with one or another type of the polymer chains, we provide a control on the nanoparticle distribution within one or another part of lamellar structure. Nanoparticles have a selective affinity to one of the blocks and self-assemble within this block during annealing. This leads to a spatially distributed ordered arrangement of the nanoparticles within the copolymer matrix.[7−10]

For the synthesis of the composite, control over the structure of the host matrix as well as over the spatial distribution of the nanoparticles inside the composite is needed. It was demonstrated that transmission electron microscopy[1−3] (TEM), secondary ion mass spectroscopy[11] (SIMS), and X-ray reflection standing wave fluorescent spectroscopy[12,13] can be used to obtain information about the distribution of nanoparticles inside the composite. Here we used neutron reflectometry, which yields simultaneously in specular reflection the depth profile and in off-specular scattering the lateral structure of the nanocomposite film. This method is nondestructive and is very sensitive to low concentrations of nanoparticles. In further studies it will be also applied to study the magnetic properties of nanocomposites using polarized neutrons. In our first experiments we used only neutron specular reflection for the investigation of lamellar composite films made of a diblock-copolymer matrix with incorporated nanoparticles.[8,9] However, it was shown that block-copolymer films create strong off-specular scattering,

* To whom correspondence may be addressed. E-mail: vlauter@ill.fr.

[†] Part of the *Langmuir* special issue dedicated to neutron reflectometry.

[‡] Technical University München.

[§] Joint Institute for Nuclear Research.

[||] Institut Laue Langevin.

[⊥] Petersburg Nuclear Physics Institute.

[#] Institut für Festkörperforschung.

(1) Möller, M.; Spatz, J. P. *Curr. Opin. Colloid Interface Sci.* **1997**, *2*, 177.

(2) Zehner, R. W.; Lopes, W. A.; Morkved, T. L.; Jaeger, H. M.; Sita, L. R. *Langmuir* **1998**, *14*, 241.

(3) Gubin, S. P. *Colloids Surf., A* **2002**, *202*, 155.

(4) Briggs, D. *Surface Analysis of Polymers by XPS and Static SIMS*; Cambridge University Press: Cambridge, 1998.

(5) Zaitsev, V.; Seo, Y.; Shin, K.; Zhang, W.; Schwarz, S.; Rafailovich, M.; Sokolov, J. *Mater. Res. Soc. Symp. Proc.* **2001**, KK6.4.

(6) Anastasiadis, S. H.; Russel, T. P.; Satija, S. K.; Majkrzak, C. F. *Phys. Rev. Lett.* **1989**, *62*, 1852.

(7) Hamdoun, B.; Ausserre, D.; Joly, S.; Gallot, Y.; Cabuil, V.; Clinard, C. *J. Phys. II* **1996**, *6*, 493.

(8) ⟩Lauter−Pasyuk, V.; Lauter, H. J.; Ausserre, D.; Gallot, Y.; Cabuil, V.; Hamdoun, B.; Kornilov, E. I. *Physica B* **1998**, *248*, 243.

(9) Lauter-Pasyuk, V.; Lauter, H. J.; Ausserre, D.; Gallot, Y.; Cabuil, V.; Kornilov, E. I.; Hamdoun, B. *Physica B* **1998**, *241−243*, 1092.

(10) Lefebure, S.; Cabuil, V.; Ausserre, D.; Paris, F.; Gallot, Y.; Lauter-Pasyuk, V. *Prog. Colloid Polym. Sci.* **1998**, *110*, 94.

(11) *Secondary Ion Mass Spectroscopy SIMS XI*; Gillen, G., Lareau, R., Bennett, J., Sterie, F., Eds.; Wiley: New York, 1998.

(12) Bedzyk, M. J.; Bommarito, G. M.; Schildkrout, J. S. *Phys. Rev. Lett.* **1989**, *62*, 1376.

(13) Lin, B.; Morkved, T. L.; Meron, M.; Huang, Zh.; Viccaro, P. J.; Jaeger, H. M.; Williams, S. M.; Schlosman, M. L. *J. Appl. Phys.* **1999**, *85*, 3180.

which should be included in the data analysis.[14−17] Also the presence of the nanoparticles can induce additional distortion of the copolymer matrix and the interfaces.

The off-specular scattering itself contains valuable information about the internal structure of the film, including the nanoparticles' distribution, lateral structure of the roughness, and its conformity though the lamellar multilayer and also the surface structure of the film. We developed a theoretical approach based on the distorted wave born approximation (DWBA), which allows for description of a full two-dimensional intensity map including the dynamical range close to the total reflection region.[16,17] The comprehensive theoretical analysis of both specular reflectivity and off-specular scattering patterns measured over a broad range of incident and scattered wave vectors delivers detailed and rather complete information on the surface topology and roughness correlation along each interface and across the multilayer stack.

In this study we investigated a composite lamellar polystyrene−poly(butyl methacrylate) P(Sd-*b*-BMA) film with a high concentration of the incorporated magnetite Fe_3O_4 nanoparticles with the average diameter of 5 nm. We succeeded in incorporating nanoparticles up to 7% of the volume fraction. As a reference, a pure P(Sd-*b*-BMA) film was investigated and the obtained parameters are compared to the ones of the composite film. From this comparison, it follows that even at high concentrations the nanoparticles stay incorporated in the film and the lamellar structure is not destroyed. Further, a periodic location of the particles in the PS layers as well as the transverse and lateral structure of lamellar pure copolymer and composite films was determined.

Experimental Details

Sample Preparation. For the sample preparation we used a nearly symmetric poly(styrene-*block-n*-butyl methacrylate) diblock copolymer, denoted P(Sd8-*b*-nBMA) with a molecular mass $M_w = 187\ 000$ g/mol, a polydispersity $M_w/M_n = 1.18$, a fully deuterated polystyrene block, and a styrene fraction of the copolymer of $f_{PSd8} = N_{PSd8}/N = 0.53$. The diblock copolymer material was prepared anionically and was obtained from the Polymer Standard Service, Mainz. The polymer−polymer interaction parameter of PS and PnBMA is $\chi = A + B/T$ with $A = -0.0357 \pm 0.002$ and $B = 17.7 \pm 1$ K, and thus during annealing the strong segregation regime is addressed.

Magnetite Fe_3O_4 nanoparticles were covered with polystyrene hairs from α-lithium polystyrene sulfonated (LPSS). At present the technology of both, the cyclohexane[18] and the toluene[10] magnetic fluid based on maghemite (Fe_2O_3), is known. However, it would be difficult to use this technology to obtain a magnetic colloid based on magnetite because of the oxidation of Fe_3O_4 to Fe_2O_3 in acid medium. The conditions for absorption of LPSS on magnetite nanoparticles were studied, and an alternative method was developed which will be published elsewhere.[19] The mean size of the nanoparticles as determined with light scattering is 5 nm with 20% variance.

(14) Lauter-Pasyuk, V.; Lauter, H. J.; Toperverg, B. P.; Nikonov, O.; Petrenko, A.; Schubert, D.; Petry, W.; Aksenov, V. *ILL Millennium Symposyum* **2001**, *59*, http://www.ill.fr/pages/menu_g/docs/ILL_Proceedings.pdf.
(15) Lauter-Pasyuk, V.; Lauter, H. J.; Toperverg, B. P.; Nikonov, O.; Petrenko, A.; Schubert, D.; Schreiber, J.; Burcin, M.; Petry, W.; Aksenov, V. *Appl. Phys. A* **2002**, 74.
(16) Toperverg, B. P.; Lauter-Pasyuk, V.; Lauter, H. J.; Nikonov, O.; Ausserre, D.; Gallot, Y. *Physica B* **2000**, *276−278*, 355.
(17) Toperverg, B. P.; Lauter-Pasyuk, V.; Lauter, H. J.; Nikonov, O.; Ausserre, D.; Gallot, Y. *Physica B* **2000**, *283*, 60.
(18) Cabuil, V.; Hochart, N.; Perzynsky, R.; Lutz, P. J. *Prog. Colloid. Polym. Sci.* **1994**, *97*, 71.
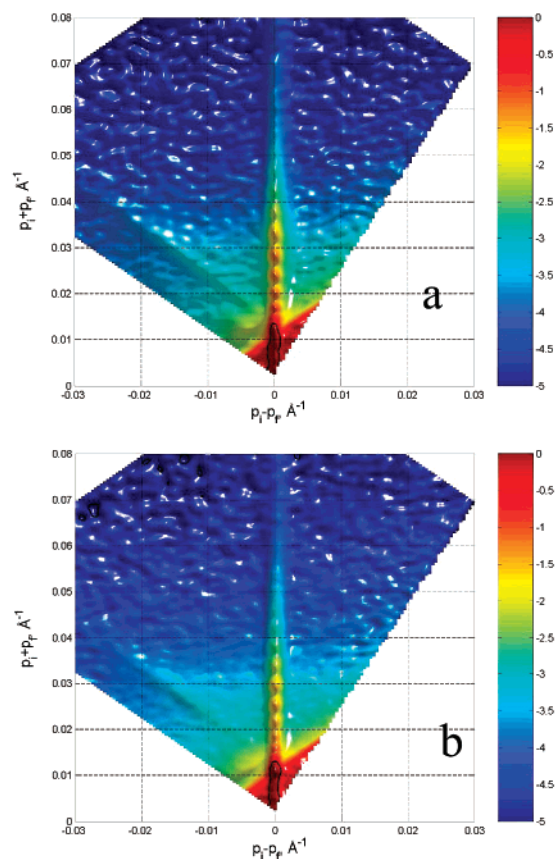(19) Gordeev, G.; Orlova, D.; Lauter-Pasyuk, V.; Lauter, H. J. In preparation.

Figure 1. Experimental two-dimensional intensity maps from the not annealed samples right after preparation of (a) the pure P(Sd-*b*-BMA) thin film and (b) the copolymer film with incorporated Fe_3O_4 nanoparticles. p_i and p_f are the perpendicular to the surface components of the incoming and outgoing neutron wave vectors, respectively. The strong intensity along the line $p_i - p_f = 0$ corresponds to the specular reflection. The Yoneda scattering intensity spreads mainly to the left from the specular line.

P(Sd8-*b*-nBMA) and hairy nanoparticles were blended in a toluene solution with a 7% volume fraction of the nanoparticles. The naturally oxide covered Si(100) surface (SILTRONIX) was cleaned before the spin coating of a thin polymeric film. The substrates were stored in an acid cleaning bath (100 mL of 80% H_2SO_4, 35 mL of H_2O_2, and 15 mL of deionized water) for 15 min at 80 °C and subsequently rinsed with deionized water until no residues from the acid bath were left. After the substrates were dried with compressed oil-free nitrogen, they were flushed with fresh toluene. After spin coating, homogeneous P(S-b-MMAd8) films containing the magnetite nanoparticles were obtained.

Atomic Force Microscopy (AFM). The AFM was used for the surface characterization of the composite diblock-copolymer/nanoparticle thin films before and after annealing. The AFM measurements were carried out with Dimention 3100 AFM microscope and NanoScope IIIa system controller (Digital Instruments, Santa Barbara, CA). The cantilevers were made of Si, and its resonance frequencies were 150−190 kHz. The measurements were performed in tapping mode (oscillating contact mode) under ambient air conditions.

Neutron Specular Reflection and Off-Specular Scattering. The experiments on neutron specular reflection and off-specular scattering were performed on the D17 reflectometer at the Institut Laue Langevin at Grenoble,[20] using the time-of-flight method with the wavelength band $\Delta\lambda$ from 2 to 20 Å and the fixed incident angle $\alpha = 1.4°$. The data were recorded with a position-sensitive detector in a wide range of incoming and outgoing wave vectors k_i and k_f.[16,17] The reflected and scattered intensities were normalized for the detector efficiency and for
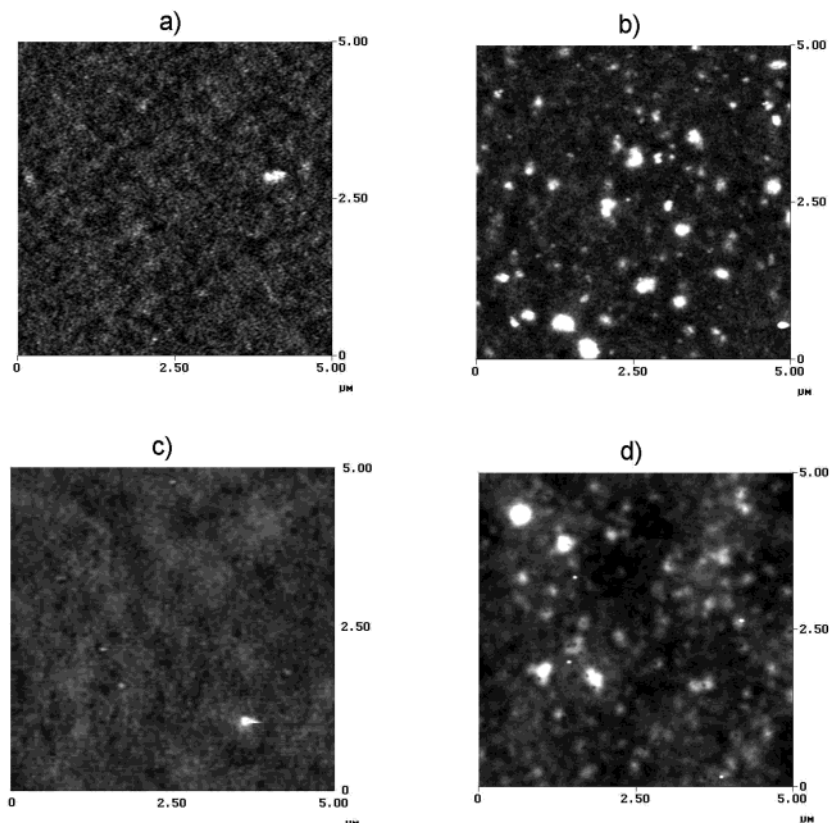
(20) http://www.ill.fr.

Figure 2. Atomic force microscope images of the not annealed samples in the as prepared state (a) of the pure copolymer film and (b) of the sample with 7% of nanoparticles. Images c and d correspond to the annealed samples. The gray scale covers a range from 0 to 12 nm.

the intensity distribution of the incident beam. The data are presented in a two-dimensional intensity map as a function of p_i and p_f, where $p_i = 2\pi \sin \alpha_i/\lambda$ and $p_f = 2\pi \sin \alpha_f/\lambda$ are the components perpendicular to the sample surface of the incoming and outgoing wave vectors, respectively.

Results and Discussion

The neutron experiment was made in two steps. First the samples with and without nanoparticles were measured in the as prepared state and then again after annealing. The reflected and scattered intensities from the samples in the as prepared state are depicted in Figure 1 as a function of $(p_i + p_f) = Q_z$ and of $(p_i - p_f)$.[15] The specular reflectivity runs along the line $p_i - p_f = 0$ and exhibits regular oscillations which are determined by the total thickness of the film. Parts a and b of Figure 1 are very similar, because in both cases before annealing we are dealing with single layers. From the periodicity of the oscillations along the specular line, the thickness of the films was determined to be 1500 ± 10 Å for the pure copolymer film and 1590 ± 10 Å for the polymer film with nanoparticles. This difference in the thickness is due to small differences in the spin-coating procedure. The off-specular intensity in a form of the Yoneda scattering[21] spreads out left from the specular intensity line indicating the presence of surface and substrate roughness. The Yoneda scattering on the right side is much less visible due to the high incident angle and the consequent loss of intensity in the range of long wavelengths in the time-of-flight experiment. The Yoneda scattering emerges from the specular line at a $Q_z = 0.0128$ Å^{-1}, which corresponds to the critical momentum transfer Q_c of the copolymer mixture with the neutron scattering length density

(NSLD) $Nb = 3.3 \times 10^{-6}$ Å^{-2} (N is the average atomic number density of the copolymer and b is its average scattering length). The average NSLD of the nanoparticles coated with nondeuterated PS is about $Nb = 3.1 \times 10^{-6}$ Å^{-2}, and therefore the Q_c values for both not annealed samples are very close. Thus, for the not annealed samples the off-specular scattering is determined by the roughness of the free surface of the copolymer films and not by the roughness of the Si substrate with $Nb = 2.073 \times 10^{-6}$ Å^{-2}, which would give a lower Q_c for the point of intersection of the Yoneda scattering with the specular line.

The AFM measurements are shown in panels a and b of Figure 2 for the as prepared state. The roughness for the pure polymer sample in Figure 2a shows a surface roughness well below 1000 Å in agreement with the Yoneda scattering in Figure 1a. The determination of the roughness for the sample with nanoparticles is perturbed by some clusters on the surface, and the slightly flatter surface (with respect to Figure 2a) is only partially detectable between the clusters. The flatter surface is also deduced from the slightly less pronounced Yoneda scattering in Figure 1b. Any effect of the clusters is not detectable in the neutron data probably due to the small density.

After annealing of the samples at a temperature $T = 165$ °C for 3 h, we repeated the measurements. Under these annealing conditions a well-ordered lamellar structure was obtained for both samples, as will be shown in the following. Further annealing did not result in any changes. The two-dimensional intensity maps from the annealed samples in panels a and b of Figure 3 are very different from the ones obtained from the as prepared samples. The specular reflected intensity shows now well-pronounced Bragg peaks. The appearance of Bragg peaks

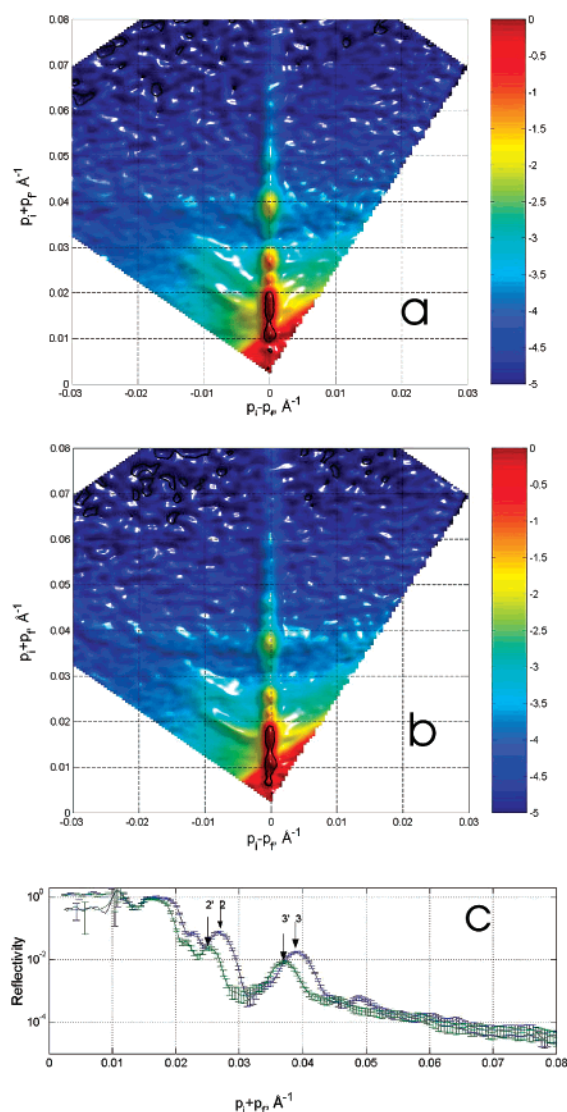(21) Yoneda, Y. *Phys. Rev.* **1963**, *63*, 455.

Figure 3. Experimental two-dimensional intensity map from the samples as in Figure 1 but after annealing during 3 h at a temperature $T = 165$ °C: (a) a pure copolymer film and (b) the sample with nanoparticles; (c) reflectivity profiles from the pure copolymer film (blue line) and the sample with nanoparticles (green line) taken as vertical cuts along the line $p_i - p_f = 0$ from parts a and b. The marks 1, 2, 3 and 1′, 2′, 3′ indicate the positions of the Bragg peaks of the pure polymer film and the film with nanoparticles, respectively.

on the reflectivity profile is caused by a multilayer structure formed by lamellae oriented parallel to the surface of the film. The presence of Bragg peaks for the sample with incorporated nanoparticles in Figure 3b proves that the multilayer structure persists and is not destroyed by a rather high concentration of the nanoparticles. The positions, Q_z^i, of the Bragg peaks are determined in the kinematic limit by the period L (PBMA–PS–PS–PBMA) of the lamellar structure with $Q_z^{i+1} - Q_z^i = 2\pi/L$. The reflectivity lines for both samples are shown together in Figure 3c. The two lines correspond to vertical cuts along the line $p_i - p_f = 0$ in parts a and b of Figure 3. The numbers 1, 2, and 3 and 1′, 2′, and 3′ correspond to the first-, second-, and third-order Bragg peaks for the samples with 0% and 7% of the nanoparticles, respectively. The multilayer structure factor regulates the relative intensities of the Bragg peaks of different orders, so that each even order is suppressed for the PBMA–PS–PS–PBMA repeating structure. The positions of the Bragg

peaks for the sample with nanoparticles are shifted toward smaller values of Q_z, proving the increase of the lamellar period L due to the presence of the nanoparticles. The reduction of intensity in the Bragg peaks indicates an increase of the interfacial roughness and changes in the NSLD due to the nanoparticles. The pattern of the off-specular scattering has also changed after the annealing. The new appearing off-specular intensity crossing the specular line in the Bragg peak positions at an right angle (so-called Bragg sheets[14−16]) is due to the interfacial roughness. This intensity appears when the roughness is correlated between different interfaces across the film. The degree of this conformity regulates the ratio between the intensity of the Bragg sheets and the intensity of the Yoneda (and super-Yoneda) scattering (the last one originates from the position of, e.g., the first-order Bragg peak). The off-specular-scattered intensities from the samples without and with nanoparticles are very similar, which proves that the interface roughness is not very much influenced by the presence of nanoparticles. This means that the critical density of nanoparticles, at which the nanoparticles will be expelled from the multilayer, is not yet reached. This critical density should be announced by an enhanced interface roughness.

The two-dimensional fit to the experimental data was performed using the model described in details earlier[14−17] and is depicted in Figure 4b for the annealed sample without nanoparticles. The experimentally determined intensity map is for comparison presented in Figure 4a. The fit along the reflectivity line reveals in the NSLD profile (see Figure 4c) that the multilayer consists of three complete layers of the PBMA–PS–PS–PBMA repeating structure marked with L. The deuteration of the PS gives a very good contrast with respect to the PBMA. So, when the two components self-organize during annealing into lamellae, then the contrast becomes apparent as shown in Figure 4c and the detailed layer structure is easy to detect with neutrons. In contrast to the samples described earlier,[14−17] the surface of the investigated multilayes was free from islands or holes as verified also with AFM (see Figure 2c). The period L was determined to 505 ± 5 Å and the thickness of the PS–PS-layers to 243 ± 5 Å.

The fit to the off-specular intensity in Figure 4b gave further information. In total there are two contributions to the off-specular scattering, one from the interfaces and one from the free surface.[15] The interfacial lateral correlation length ξ, which is the average lateral length over which the interface between the PS and PBMA lamellae is "flat", was determined to be $\xi = 3000 \pm 50$ Å. The root mean square height of the roughness is $\sigma = 20 \pm 5$ Å, which gives a scale of how much the PS and PBMA interface fluctuates. A further parameter is the conformity parameter $\zeta = 6$. It means in a simplified view that starting from one interface a roughness event is still noticeable at a distance of six interfaces further away. Further the fit shows that the lateral correlation at the free surface is 4000 ± 500 Å, which is in agreement with the AFM measurement (see Figure 2c). It should be noted that the roughness from the free surface contributes only to the Yoneda scattering.

The sample with nanoparticles was analyzed with the same model, and the result of the fit to the data shown in Figure 5a is depicted in Figure 5b. Cuts along the specular lines taken from panels a and b of Figure 5 are presented in Figure 5c, showing the quality of the fit. The corresponding NSLD profile is shown in Figure 5e. The multilayer structure is modified with respect to Figure 4c by the following effects. As the thickness and NSLD of the PBMA layers are not changed, the PS–PS layers are
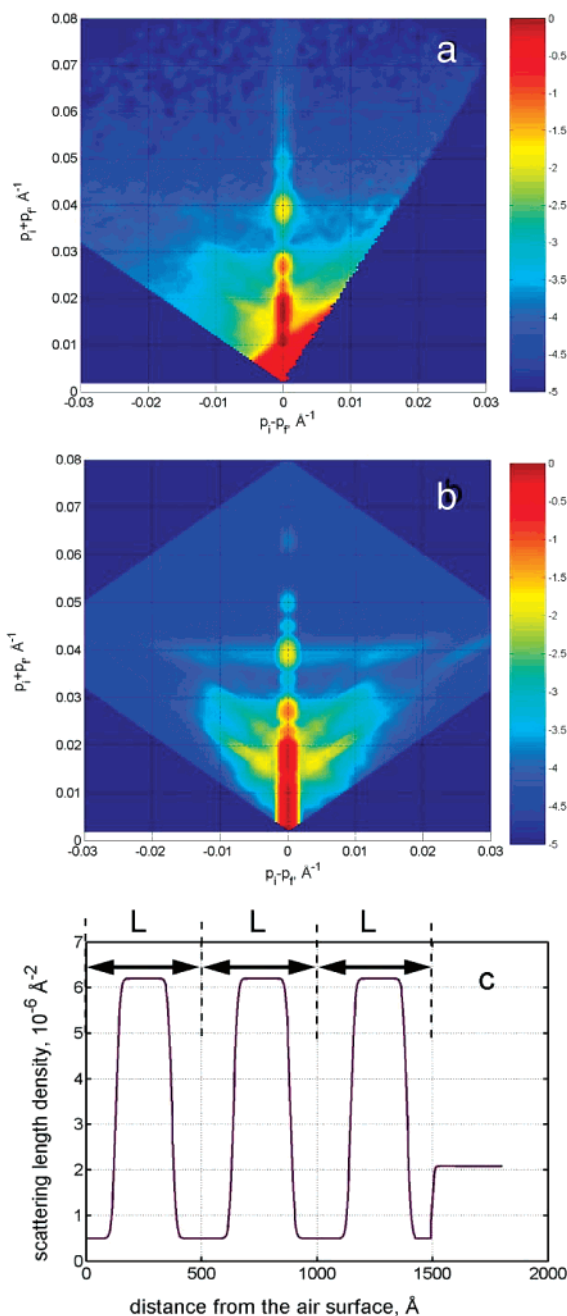
Figure 4. Experimentally measured (a) and theoretically modeled (b) intensity map of the specular reflection and off-specular scattering from the annealed sample of pure P(Sd-*b*-BMA) copolymer film. (c) Neutron scattering length density profile as a function of the distance from the free surface extracted from the model fit to the data, showing the three-layer lamellar structure of the film. *L* is the repeating period; parameters of the lateral and the transverse roughness fluctuations obtained from the fit to the data are described in the text.

swollen and show a reduced NSLD. The changes in the PS layers are due to the presence of the nanoparticles. Thus the nanoparticles organize into the PS layers and the PBMA layers do not host nanoparticles. The repeating length L increases to $L = 535 \pm 10$ Å, which is only due to the increase of the thickness of the PS lamellae showing now a value of 273 ± 10 Å. This corresponds to an increase of about 12% of the PS thickness due to the 14% volume fraction (with respect to PS) of coated nanoparticles. In accordance, the NSLD of the PS layers shown in Figure 5e has a by 14% lower potential with respect to the NSLD
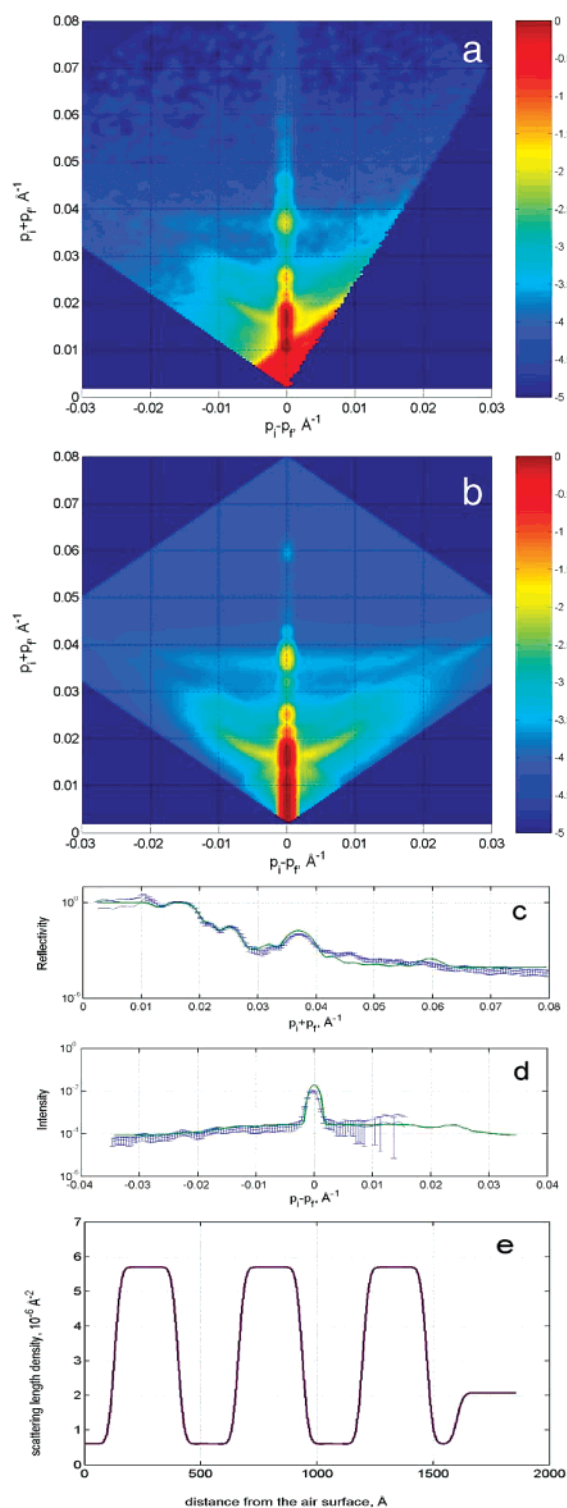

Figure 5. Experimental (a) and theoretical (b) intensity maps of the specular reflection and off-specular scattering from the annealed polymer sample with nanoparticles. Experimental and theoretical (c) reflectivity profiles and (d) horizontal cuts through the third-order Bragg sheet scattering extracted from figures a and b. (e) Neutron scattering length density profile as a function of the distance from the free surface obtained from the model fit to the data, showing a three-layer lamellar structure of the film as in Figure 3c but with increased thickness and reduced NSLD of the PS layers due to the presence of the nanoparticles.

of the pure PS in Figure 4c. The off-specular scattering from the interfaces is characterized by an increased root mean square roughness $\sigma = 30 \pm 5$ Å combined with a

reduced lateral correlation length of 2400 ± 50 Å. The conformity parameter dropped to $\zeta = 3$, so the interface roughness correlation reaching nearly throughout the multilayer without nanoparticles is now practically reduced to half of the multilayer.

The surface roughness shows with an enhanced lateral correlation length $\xi = 10000 \pm 500$ Å, an effect which is also visible in Figure 2d in the AFM measurement.

Summary

We performed a detailed study of a new composite lamellar film with a high concentration of the nanoparticles and compared the parameters of the film to the ones of a film without nanoparticles. It is shown that the P(Sd-*b*-BMA) copolymer multilayer orders the assembly of PS-coated nanoparticles into the lamellar array consisting of PS and PBMA lamellae and more precisely into the PS–PS bilayers of this host matrix. The application of neutron specular reflection and off-specular scattering accompanied by a two-dimensional data analysis allows for a detailed description of the nanoparticles distribution inside the copolymer matrix. As a result, the parameters of the transverse and the lateral structure for the pure copolymer film and for the composite film are obtained.

The interface roughness parameters can be taken as a measure whether the concentration of the nanoparticles reaches its limits. The essential effect is that the correlation of the interface roughness reduces, which is certainly not crucial for an expulsion of the nanoparticels or for the stability of the multilayer. The other interface and surface roughness parameters indicate that still more nanoparticles can be incorporated in order to enhance, e.g., the expected magnetic behavior of the composite film through the nanoparticle concentration.

LA026818A